Stick–slip motion and controlled filling speed by the geometric design of soft micro-channels

Journal of Colloid and Interface Science 524 (2018) 139–147

Contents lists available at ScienceDirect

Journal of Colloid and Interface Science

journal homepage: www.elsevier.com/locate/jcis

Regular Article

Stick–slip motion and controlled filling speed by the geometric design of soft micro-channels

Johanna Andersson, Anette Larsson, Anna Ström *

Department of Chemistry and Chemical Engineering, Chalmers University of Technology, Gothenburg, Sweden
SuMo Biomaterials, VINN Excellence Centre, Chalmers University of Technology, Gothenburg, Sweden

GRAPHICAL ABSTRACT

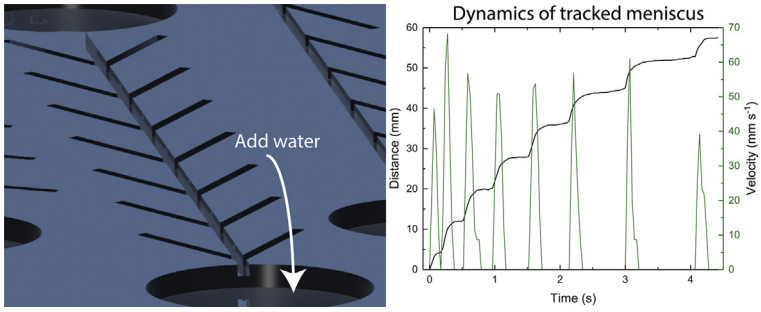

ARTICLE INFO

Article history:
Received 30 January 2018
Revised 20 March 2018
Accepted 21 March 2018
Available online 22 March 2018

Keywords:
Foam structures
Pinning meniscus
Lucas–Washburn equation
Capillary action

ABSTRACT

Hypothesis: Liquid can move by capillary action through interconnected porous materials, as in fabric or paper towels. Today mass transport is controlled by chemical modification. It is, however, possible to direct mass transport by geometrical modifications. It is here proposed that it is possible to tailor capillary flow speed in a model system of micro-channels by the angle, size and position of attached side channels.

Experiments: A flexible, rapid, and cost-effective method is used to produce micro-channels in gels. It involves 3D-printed moulds in which gels are cast. Open channels of micrometre size with several side channels on either one or two sides are produced with tilting angles of 10–170°. On a horizontal plane the meniscus of water driven by surface tension is tracked in the main channel.

Findings: The presence of side channels on one side slowed down the speed of the meniscus in the main channel least. Channels having side channels on both sides with tilting angles of up to 30° indicated tremendously slower flow, and the liquid exhibited a stick-slip motion. Broader side channels decreased the speed more than thinner ones, as suggested by the hypothesis. Inertial forces are suggested to be important in branched channel systems studied here.

1. Introduction

The spreading or moving of fluids is of great industrial importance, for example, in oil recovery, textile processing, and mortar drying, and knowledge of it is also needed in various biomedical applications and diagnostics, such as lab on a chip or lab on a paper [1]. The spreading of water on hydrophilic non-smooth surfaces also occurs naturally in biology and has important functions, for example, in ensuring effective nutritional absorption and the perception of tastes and odours [2].

* Corresponding author.
E-mail address: anna.strom@chalmers.se (A. Ström).

https://doi.org/10.1016/j.jcis.2018.03.070
0021-9797/

A fluid can be moved, for example, in microfluidics, using valves and pumps requiring active work and careful adjustment of the pressure. It needs experienced and skilled personal for Lab-on-a-chip-devices to adjust those parameters to apply an appropriate pressure, which could be rare specifically in developing countries [3]. An easier way to move fluids is to take advantage of capillary action and passively let the liquid flow. Capillary action, or wicking, is driven by the surface forces of the material and the imbibing liquid, and occurs spontaneously when (i) the contact angle between the imbibing liquid and the surface is <90° and (ii) the diameter of the capillary/channel is small enough [4]. Capillary action has been studied and modelled by Lucas [5] and Washburn [6] and can be described by the commonly quoted Lucas–Washburn (LW) equation, which combines the driving force (i.e., capillary pressure) with the opposing Poisseuille flow:

$$x^2 = \frac{\gamma R \cos\theta}{2\mu} t \quad (1)$$

where R is the channel radius, μ the dynamic viscosity of the liquid phase, γ the surface tension of the liquid, and θ the static contact angle of the liquid on the channel wall [5,6].

Wicking and wetting in hard 2D materials are well understood through models and theories [7,8]. Several studies of wicking in differently shaped channels (i.e., V-shaped [9,10], rectangular [11], skewed U-shaped [12], and cylindrical [11]) demonstrate that wicking generally follows LW predictions independent of whether the channels are closed or open. The fluid direction can be controlled by using pillars on a plane (see [13], a numerical study). Wicking in the preferred direction can also be obtained by manipulating the design of structures extending into the channels [14]. The wicking of fluid in open channels offers the advantages of ease of surface modification, ease of cleaning (or, as in the present case, use of disposable systems), and reduced risk of clogging [11]. The only way of filling open channels is by using capillary action and/or wicking, since they cannot be filled by pumping. Although paper-based medical devices hold great potential, they still vary in specificity and sensitivity [1]. Generally only about 50% of the applied test fluid reach the detection zones and their speed greatly influences both specificity and sensitivity. These are still issues to overcome, where the understanding of precise flow dynamics could help to add to the breakthrough of Lab-on-a-paper-devices [3].

Preferred pathways of the imbibing liquid are also observed in interconnected 3D materials characterised by inhomogeneous pore size distributions, such as the paper or sponges used in wound-care products [15–17]. Pore sizes are often hierarchical in that there are pores which can differ one or several magnitudes in size. The exact cause of these preferred pathways is discussed in the literature but is not yet known. One point of discussion has been if large or small pores are filled first in an interconnected porous system [18–21]. Since the liquid flows faster in larger capillaries one can assume that they are also filled first in a porous system. However, capillary pressure is higher in smaller pores so that liquid can also rise higher than in thicker capillaries.

Moreover, in an interconnected porous system, the liquid not only takes a preferred pathway but also moves discontinuously. This means that the meniscus accelerates and decelerates throughout the system, giving rise to increased inertial forces [20] adding up to behaviour deviating from LW equation predictions [17,22]. Sometimes, the liquid even stops and then suddenly resumes movement in what are referred to as Haines jumps [23].

The challenge of investigating such a complex porous system is that of directly tracking several menisci in a 3D porous system. However, systematic studies seeking the cause of such preferred pathways might fail because of the high production costs of precisely defined channels. Channels with controlled size and structures are commonly prepared using photolithography techniques. Photolithography involves the deposition of photoresist on a substrate using a spin coater, and then the manufacture of a master used in exposing the photoresist to UV light with a mask aligner. This causes the photoresist to cross-link in the exposed or non-exposed areas, depending on the type of resist; the resist is subsequently lifted off by a remover. All the involved work must be undertaken in cleanroom facilities. While such techniques allow precise control of the channels, they are costly and time consuming. A low-cost alternative to the lab-on-a-chip approach is the application of microfluidics on paper in the lab-on-a-paper approach [1,24]. Photolithography (which physically blocks the pores in the paper), ink-jet printing (which chemically modifies the fibre structure), and wax printing (which physically deposits reagent on the fibre surface) are used to control fluid movement in lab-on-a-paper applications.

Wetting and therefore wicking are more complex in soft materials than hard materials [25,26] because local deformation of the soft material occurs near the contact line [27,28]. We have previously reported that capillary filling in soft hydrophilic capillaries is in line with the LW equation, although at a slower rate than in, for example, glass capillaries [29]. The controlled wicking of fluid in soft materials, such as gels, is of great importance as such systems are used in microfluidic applications for diagnostics [30,31]. Silva et al. reported a stick–slip motion occurring in glass capillaries coated with a dried hydrogel [32]: as the meniscus advanced, it became successively pinned and unpinned due to swelling and local deformation, indicating that substrate deformation significantly affects the contact-line dynamics of the liquid movement. From a broader perspective, not only gels are soft, but also often foams and various types of paper, comprising a vast range of materials and applications. Gel applications have some advantages over lab-on-a-paper applications, such as transparency, non-toxicity, and biocompatibility with cells. Despite their relatively short shelf life, polysaccharides are a cheap, renewable, and readily available material. Fluid wicking in soft hydrophilic materials of various geometric shapes has been much less studied than wicking in hard channels.

Here we report on wicking speed within geometrically structured soft materials obtained using 3D-printed moulds in which a hydrogel (i.e., calcium alginate) was allowed to cure. This method results in channels with rectangular cross-sections and open top sides. We can control the wicking speed of an imbibing fluid in a main channel by varying the tilting angle and position of side channels. The width of the side channels are varied to investigate if small or large pores are filled first. The use of 3D-printed moulds in combination with curable hydrogels opens up the possibility of the rapid, cheap, and simple use of variously structured materials in which the controlled wicking of fluid is obtained.

2. Method and materials

2.1. Drawing of a 3D mould

An overview of the process of fabricating microchannels (μ-channels) in gels is shown in Fig. 1. A mould was drawn in 3D using AutoCAD (Version 2014; Autodesk, San Rafael, CA, USA). Reservoirs for depositing the liquid were designed to hold sufficient liquid volume to fill at least the entire channel.

The mould was designed with side channels added on one or two sides of a main flow channel with varying tilting angles and widths (see Fig. 2). The sketch shows a top view of part of a channel. As the junctions, we define the point in the main channel where the side channels are connected to the main channel. The

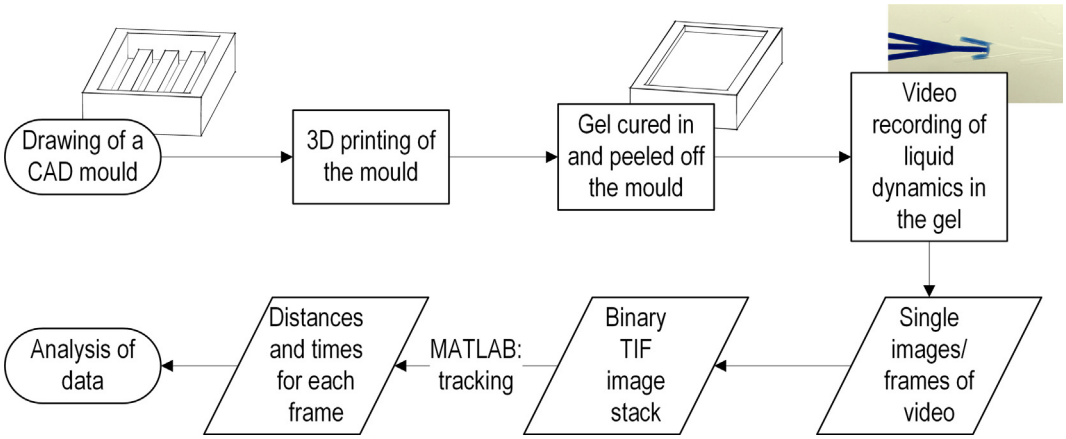

Fig. 1. Flowchart of the process of producing μ-channels in semi-solids.

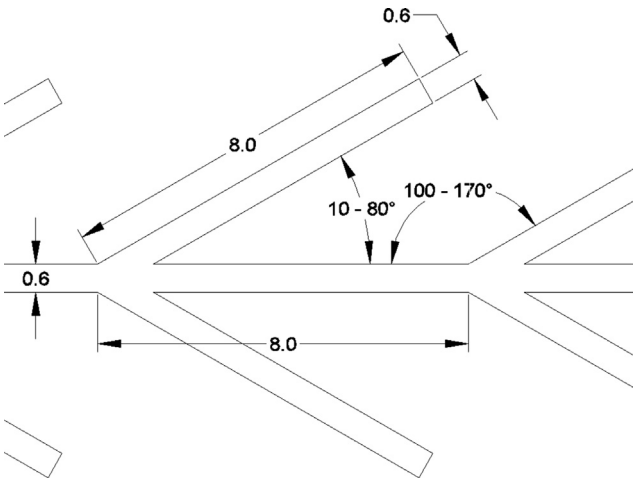

Fig. 2. Channel design. The angles of the side channels were varied from 10° to 170°, with angles <90° defined relative to liquid coming from the left and angles >90° relative to liquid from the right (sharp angles); dimensions given in mm.

width and height of the channels was 0.6 mm and the angles tested were 10°, 30°, 60°, and 80° and, using the same mould but the opposite flow direction, also 100°, 120°, 150°, and 170°. Moreover, the influence of side-channel width was tested with channels 0.3, 0.4, and 0.6 mm wide having angles of 30°, 80°, 100°, and 150° with respect to the main channel.

The mould was 3D printed by Shapeways (New York, NY, USA) in a material called Frosted Ultra Detail,[1] a UV-cured acrylic polymer heat resistant up to 80 °C. The roughness of the mould is not expected to influence the flow (details in Supplementary information).

2.2. Gel preparation, curing, and recording

An aqueous alginate solution containing 2% w/w alginate (kindly provided by FMC Biopolymer, Girvan, UK) was prepared by adding alginate at room temperature (RT) under vigorous stirring. The dispersion was then heated to 80 °C for 30 min, after which it was left to cool to RT and the pH was adjusted to 7. Immediately before gel preparation, the alginate solution was deaerated under vacuum for approximately 15 min. Controlled gel formation was achieved by mixing calcium carbonate ($CaCO_3$; Provencale SA, Brignoles, France) and D-(+)-glucono-δ-lactone (GDL; Sigma-Aldrich, Darmstadt, Germany) in water just before adding the alginate solution to yield a final alginate concentration of 1.7% w/w. The mixture was without delay poured into the 3D-printed mould and left to gel for 24 h at RT in a closed chamber with a relative humidity of 98%, controlled by saturated salt solutions of potassium sulphate (K_2SO_4; Merck Millipore, Burlington, MA, USA). The stoichiometric relationship of calcium ions to G units (i.e., the calcium-binding copolymer of the alginate chains) was 1.0.

Next, the gel was removed from the mould (it released easily) and the wicking process was videotaped. No visual deviation from the initial mould was observed in the final structure obtained in the alginate gel. Filtered ultra-pure water stained with methylene blue (Fluka Chemie, Buchs, Switzerland) was added to the reservoir with a pipette. The liquid penetrated the channel and the process was recorded with a camera (EX-ZR300; Casio, Tokyo, Japan). For reproducibility, each gel was used only once, though in principle a gel could be used several times. Each experiment was conducted in at least four replicates.

2.3. Data post processing

Using the software FFmpeg (version N-54571-g00b1401), the videos were divided into single images. The images in which the liquid penetrates one channel were selected and compiled to form a stack of TIF images using ImageJ (version 1.50b). Using the same software, the area of interest was cropped, the contrast between liquid and gel was increased by selecting only the red channel of the images, and finally the image stack was converted into binary images. A MATLAB (version R2015b) code was written to track the liquid position in each image, with the (known) total length of the channel being used to convert the image resolution to metric units. The volume flow was calculated by counting the amount of black pixels, which depicted the stained water, and relating it to the volume of the channel (see Supplementary information on further details).

3. Results and discussion

We used a versatile, simple, and rapid method to fabricate μ-channels. The side channels varied in tilting angle from the main channel and in their width. In this study, we investigated the wicking speed of water into channels cast in calcium alginate gel. Wicking tests were performed by adding a precise amount of stained water to the reservoir and then analysing the position of the water front using a high-speed camera. By careful post processing of the

[1] The reader is referred to the producer's homepage (http://www.shapeways.com) for further details on the material, resolution (hundredths of micrometre), and printing limitations.

videos, the distance the meniscus travelled over time was determined. It should be noted that the contact angle between the water and alginate gel was very low leading to a rapid spreading of water over the gel. Capillary flow into gels with straight channels and circular cross-sections follow the typical behaviour of LW but tend to be slower compared to hard materials [29]. The structure of the gel has been described elsewhere [33,34] and is typical for a polyelectrolyte gel i.e., with large variation in pore sizes. The interaction between the fluid and the gel is considered insignificant at the timescales relevant for this study, as swelling occurs at longer timescales [35], previously discussed in similar systems [29]. The reader is referred to the Video S1 in the supplementary materials showing typical imbibition behaviour in real-time in channels with various tilting angles of the side channels and close-up videos of the junctions.

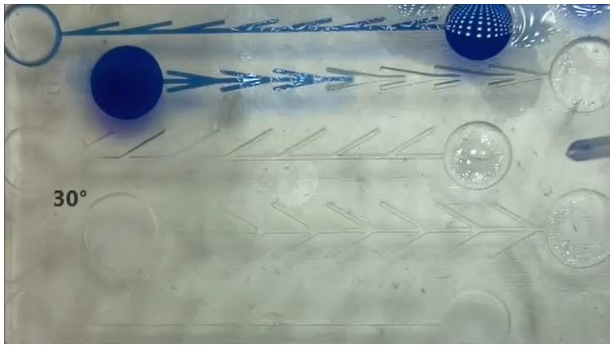

Video S1.

3.1. Stick–slip motion is obtained in branched channels

We investigated the position of the meniscus over time in the main channel without considering the side channels. As a reference, we used a straight channel without any branches and having the same width. Representative results are plotted in Fig. 3. In channels about 60 mm long, the travelled distance is plotted over time for straight channels without any branches (blue line), channels having a branch on only one side (black line), and channels having branches on both sides (red line). This is shown for structures with side channels at tilting angles of (a) 10°, (b) 80°, (c) 150°, and (d) 170°.

As the blue lines in Fig. 3 indicate, the straight channel exhibited the fastest dynamics, with the whole channel being filled in under 2 s, followed by the channels with branches on one side and then the channels with branches on both sides. Such behaviour was observed independent of the angle of the side branches.

The increased time required for the liquid to travel along the whole channel with branches on one or two sides is explained by repetitive stops made by the liquid, as shown by the staircase-like patterns of distance travelled over time (Fig. 3). After a stop, the liquid resumed flowing, no sudden jump (i.e., Haines jump) being observed. The repetitive stops made by the liquid were particularly noticeable in the case of channels on both sides of the main channel and occur at each junction. The stopping of the wicking fluid can be explained by a sudden reduction in capillary pressure. As the meniscus encounters a junction, it cannot follow any walls and suddenly encounters a gap; this influences the curved meniscus in such a way that the driving force of the capillary transport of the liquid declines to zero, and the meniscus stops advancing. In the case of a channel on one side, the capillary pressure is reduced but still acts between one wall and the bottom surface. This effect was also described by Kusumaatmaja et al., who found that local pinning can temporarily hold the capillary front while the interface/meniscus advances along another side wall or bottom plate [36].

3.2. Tilting angle of the side channels accentuates the stick–slip motion

Given that the advancing curved meniscus requires channel walls between which capillary pressure can take effect, it was expected that the stop duration would be related to the time required for the side channels to fill (and therefore also be related to the volume/width of the side channels). This was not observed at all times, however, and the possible reasons for this observation will be discussed in more detail later.

Investigation of the effect of the tilting angles of the side channels on the filling time of the main channel revealed that reducing the angle increased the filling time in the design with channels on both sides. Side channels of 10° followed by 30° resulted in the absolute longest filling times for an entire channel (see Fig. 3a compared with b, c, and d) in geometries in which the side channels are tilted 80°, 150°, and 170°, respectively. It is worth noting that the geometry in Fig. 3a (with a tilting angle of 10°) and d (with a tilting angle of 170°) is exactly the same, in the sense that the side channels are tilted to the same degree, but with the difference that the side channels are tilted either against (as in a at 10°) or with the wicking direction (as in d at 170°). The design of structures in which the angle of the side channels is tilted against or with the wicking direction will substantially affect the time required for a liquid to fill an entire channel. In this case, when comparing 10° and 170°, we observe that it took 15 and 5 s, respectively, to fill the entire main channel, i.e., a threefold difference in time. Accordingly, by choosing the flow direction, the flow speed can be either fast for high angles or slow for low angles; in this way, it is possible to tailor the desired flow speed. While a reduced total filling time was observed when side channels were introduced on one side, the angle of these side channels was found to have no effect. In these cases, filling times were 3–4 s independent of the tilting angle of the side channels (i.e., 10°–170°).

3.3. Stopping time is related to travelled distance in channel

As the tilting angle of a side channel on one side had no observed impact, the rest of the study focused on the design with side channels on both sides. The stop duration at each junction (i.e., junctions 1–7) was analysed by calculating the velocity from the travelled distance and time, with the duration during which the velocity was zero being defined as a "stop". This was done by calculating the difference in distance and time between single recorded images. Below a defined threshold of 5–20 mm s^{-1}, we set the velocity to zero ("modified"), using a moving average smoothing filter for the experiments when needed. The results are peaks between which the velocity $v = 0$. An example is presented in Fig. 4, which shows the original data from one experiment for the distance travelled over time in a channel with branches of 170° (black line) and the resulting modified and smoothed velocity (green line), with the threshold velocity being set to 15 mm s^{-1} and a smoothing span of 2 values. The threshold velocity and smoothing span were adjusted and optimised for each experiment. The stopping duration was calculated as Δt where $v = 0$. The result is presented in Fig. 5, which shows the mean duration of each stop the liquid takes at each junction, with the step number denoting the first, second, third junction, etc.

As can be seen, the stop duration increases towards the end of the capillary. The increase in stop duration with successive junctions can be explained by the reduced speed of the meniscus towards the end of the capillary (Fig. 3, blue line). The declining speed of the wicking fluid is in line with the LW equation [5,6],

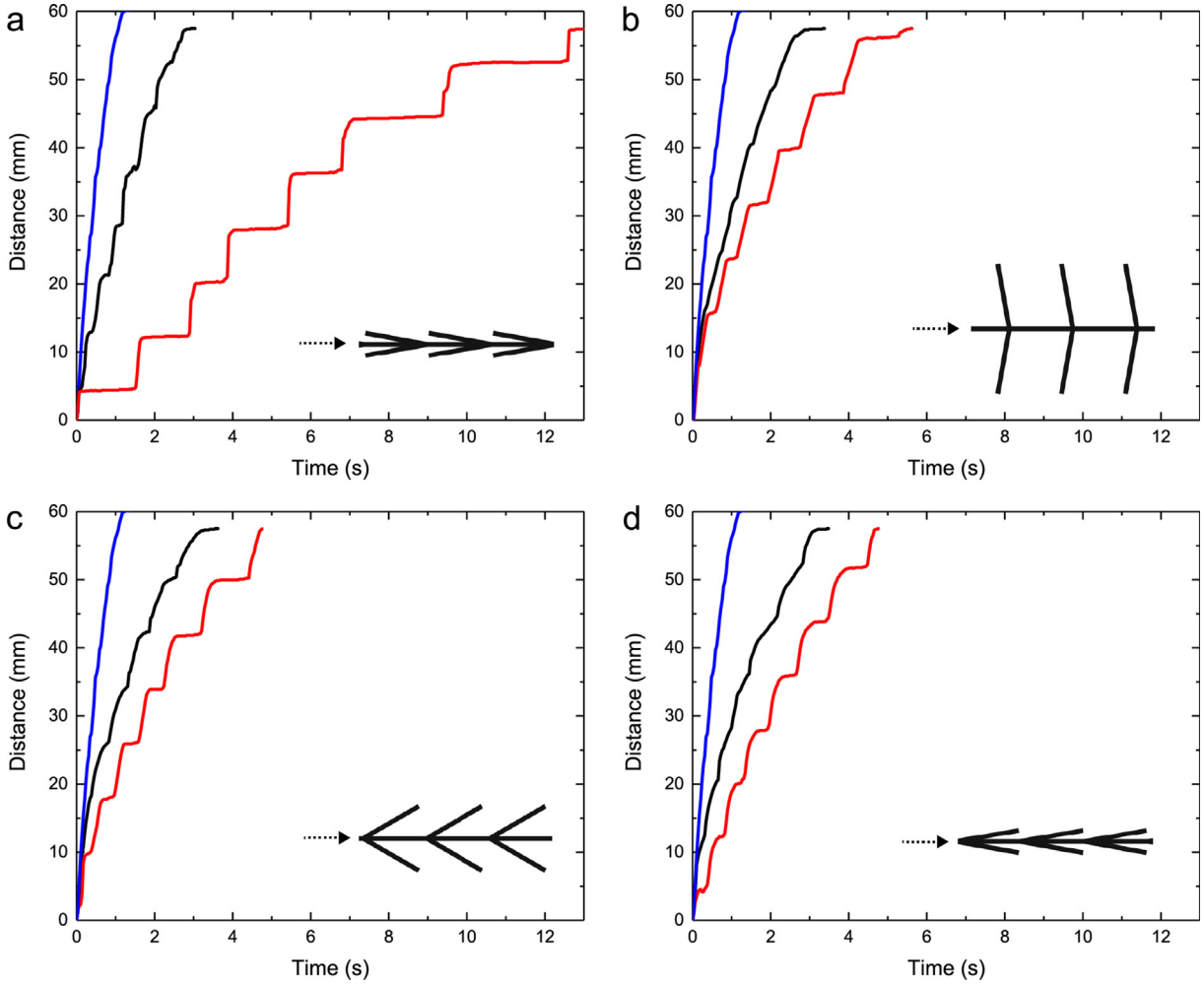

Fig. 3. Distance of liquid flow over time in channels without branches (blue), with branches on only one side (black), and with branches on both sides (red). The angles of the branches are (a) 10°, (b) 80°, (c) 150°, and (d) 170°. Note that the blue line is based on the same data in all four graphs. (For interpretation of the references to colour in this figure legend, the reader is referred to the web version of this article.)

stating a relationship of $l \propto \sqrt{t}$, where l is the travelled distance and t the time. The relationship has been reconfirmed by numerous studies of different channel geometries and sizes [4,11,37–40] and is related to the counteracting force originating from the viscous drag of the Poiseuille flow [5,6].

The inertia of the fluid is not accounted for in the original LW equation. Bosanquet [41] proposed a modified version of the LW equation in which inertia was included, a modification further developed by Ridgway et al. [15]. In the system studied here it is suggested that inertial forces are important specifically in channel geometries with long stopping times. In contrast to straight unbranched channels where inertia is only of importance during the very first milliseconds as the liquid enters the channel. [29]. However, given that the velocity is largely alternating in the branched-channel system studied here (Fig. 4), inertia will have a larger impact than in an unbranched channel. This reasoning is supported by the fact that the velocity between the junctions is slightly lower in the branched channels than over the same distance in a straight channel as shown in Fig. 6 where the velocity in a straight channel (a) is compared to the velocity of the fluid in a branched channel (b).

The velocity of the liquid between the junctions was therefore further analysed by fitting a linear curve of the distance travelled over time to each step in the graph and comparing the resulting slope of each step with the velocity in a straight channel at the same point (see Fig. 6). For clarity, we picked three representative curves, for 60°, 80°, and 150°. Both graphs show declining velocity

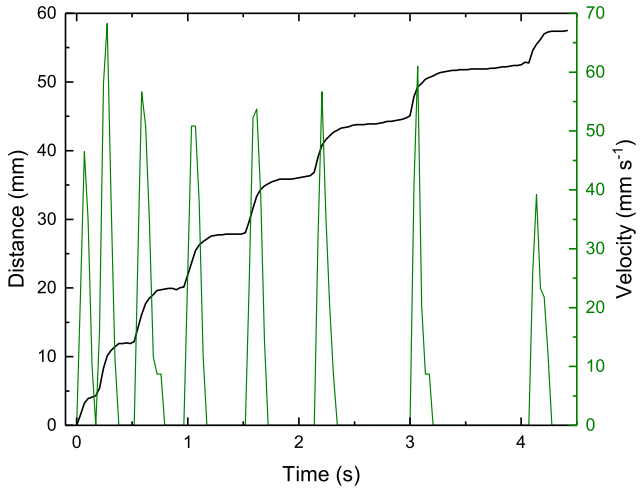

Fig. 4. Example of an experiment with branches on both sides at tilting angles of 170° showing the distance liquid travelled over time (black line) and the modified and smoothed velocity (green line). (For interpretation of the references to colour in this figure legend, the reader is referred to the web version of this article.)

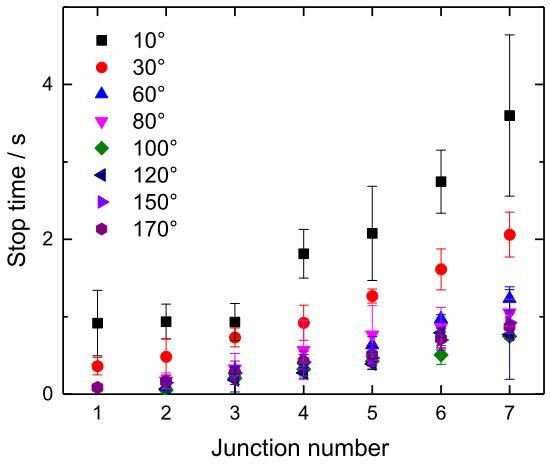

Fig. 5. Mean stopping duration of the liquid in capillaries with side channels on both sides with tilting angles as indicated in the graph. The junction number indicates the number of the side channel along the capillary.

over distance, which is related to the viscous braking of the Poiseuille flow in LW, as discussed above. However, the decline in velocity was less pronounced once the fluid had passed the very first junction in the branched channel (b) than after it had travelled the same distance in the channel without side branches (a).

While the channel width was the same, the velocity was lower in the branched channel (Fig. 6b), specifically at the beginning of the capillary, than in the unbranched one (Fig. 6a). Therefore, either the existence of the already-filled branches slowed the advancing liquid meniscus due to viscous forces, or the velocity decreased because of increased inertial forces due to the many stops. Studies are being undertaken investigating the effect of momentum on branched channel systems having different geometries at the same total volume. The volume flow was calculated from the amount of pixels in the binary images. The results indicated that, similarly to the speed in the main channel, the volume flow is not constant, but moves fastest in the beginning and is influenced by the junctions. The values range from 5 up to 40 $mm^3\ s^{-1}$ depending on the time and the geometry of the channel, see the Supplementary information for further details. This, again, strengthens the suggestion that inertial forces are important in channels with side channels, which could be the case in wicking in, for example, foams or other porous structures. However, our channels are large compared to other porous systems, they are therefore more prone to inertial forces than was a system with similar geometry studied by Feng and Rothstein [14]. The relatively large channels and the inherently greater momentum of the fluid in the present system might also explain why Haines jumps were not observed.

Another aspect visible in Fig. 5 is that the presence of channels with branches of 10° or 30° resulted in relatively long stop times compared with the other angles, where no difference in stop time was observed in channels with side channels tilted >60° (angles up to 170° were tested) (Fig. 5). To understand the effect of 10° and 30° tilting angles in delaying the wicking of the liquid, we recorded close-up videos of a junction where the side channels were tilted by 10° (Fig. 7). We observed that the stained liquid stopped at the sharp angle of the side channel.

The driving force of wicking, i.e., the concave meniscus, was missing as the liquid reached the junction. To continue flowing the liquid has to overcome a convex meniscus at the edge of the junction, where the driving force is naturally backwards. The liquid entered the side branches because the distance between the walls was the shortest in that area while the capillary pressure was highest; it filled the side channels first and then proceeded farther along the walls until the centre of the junction was finally filled. The timeline at the bottom of the figure indicates the time interval within which the images were selected. The liquid stopped for a relatively long time (a–d) when the side channels were filling, whereas the rest of the junction filled rapidly in comparison. Moving the opposite direction in the channel, the liquid never encountered such sharp edges, explaining why such movement was considerably faster. Our results are in line with observations made by Feng and Rothstein, even though their study regarded wicking of isopropanol and water in polydimethylsiloxane structures slightly differing in geometry and of smaller channel sizes [14].

3.4. Stick–slip motion is accentuated by the use of broader side channels

Given that the capillary pressure is higher in smaller channels, we investigated the effect of the side-channel width on the

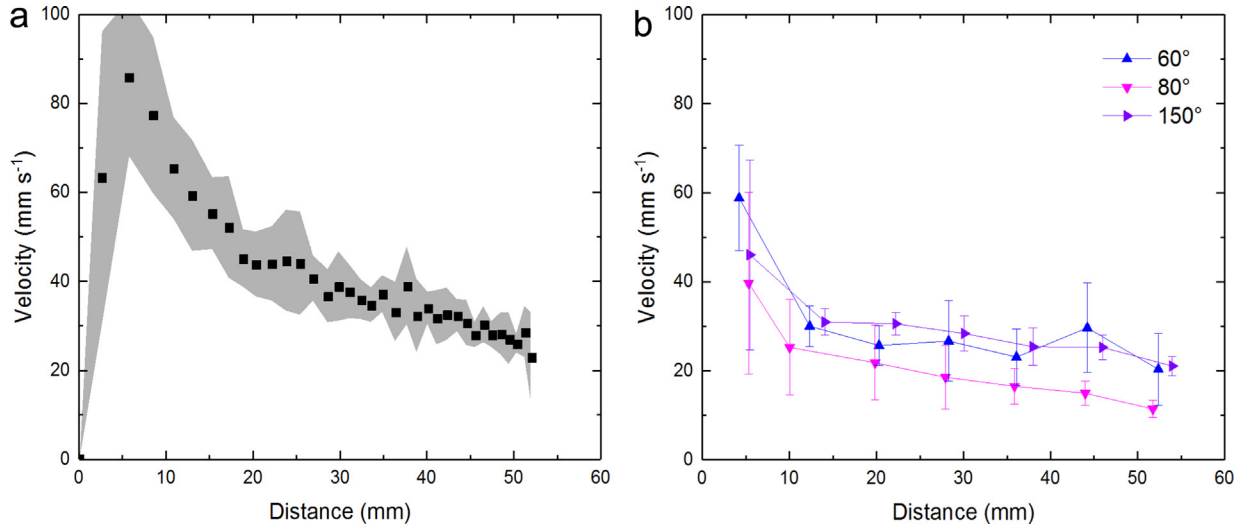

Fig. 6. (a) Mean velocity in an unbranched channel over distance; the shaded areas represent the standard deviation. (b) Velocity at each junction over distance for channels with branches on both sides with angles as indicated in the graph; three representative curves.

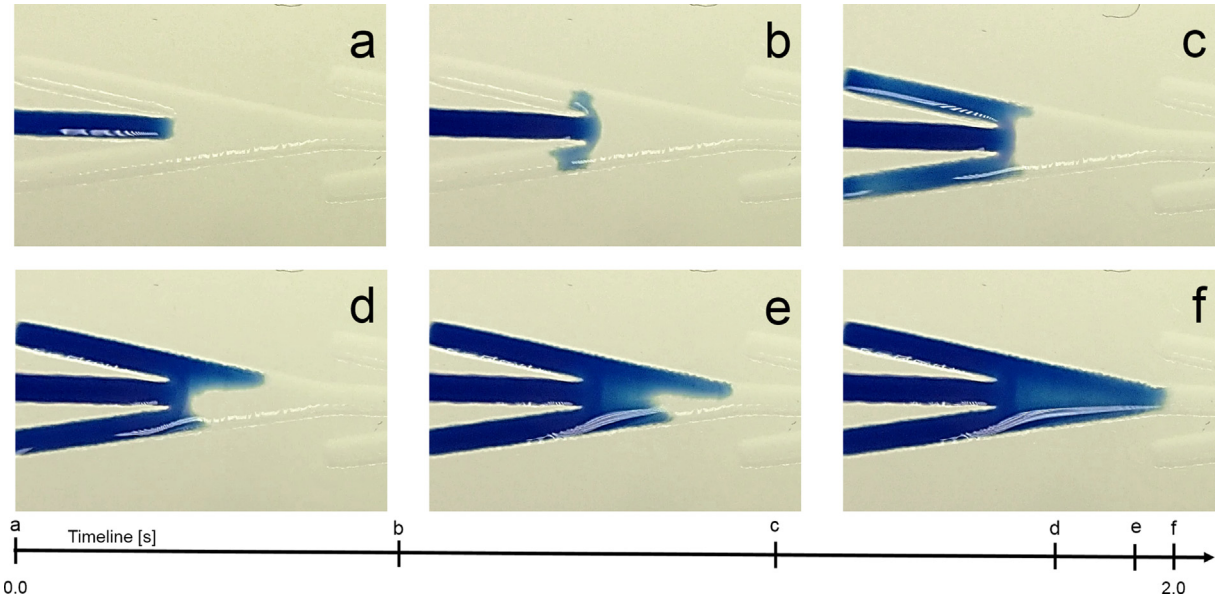

Fig. 7. Image series visualising the liquid penetration behaviour at a junction with branches of 10°; the timeline indicates the timing of the images.

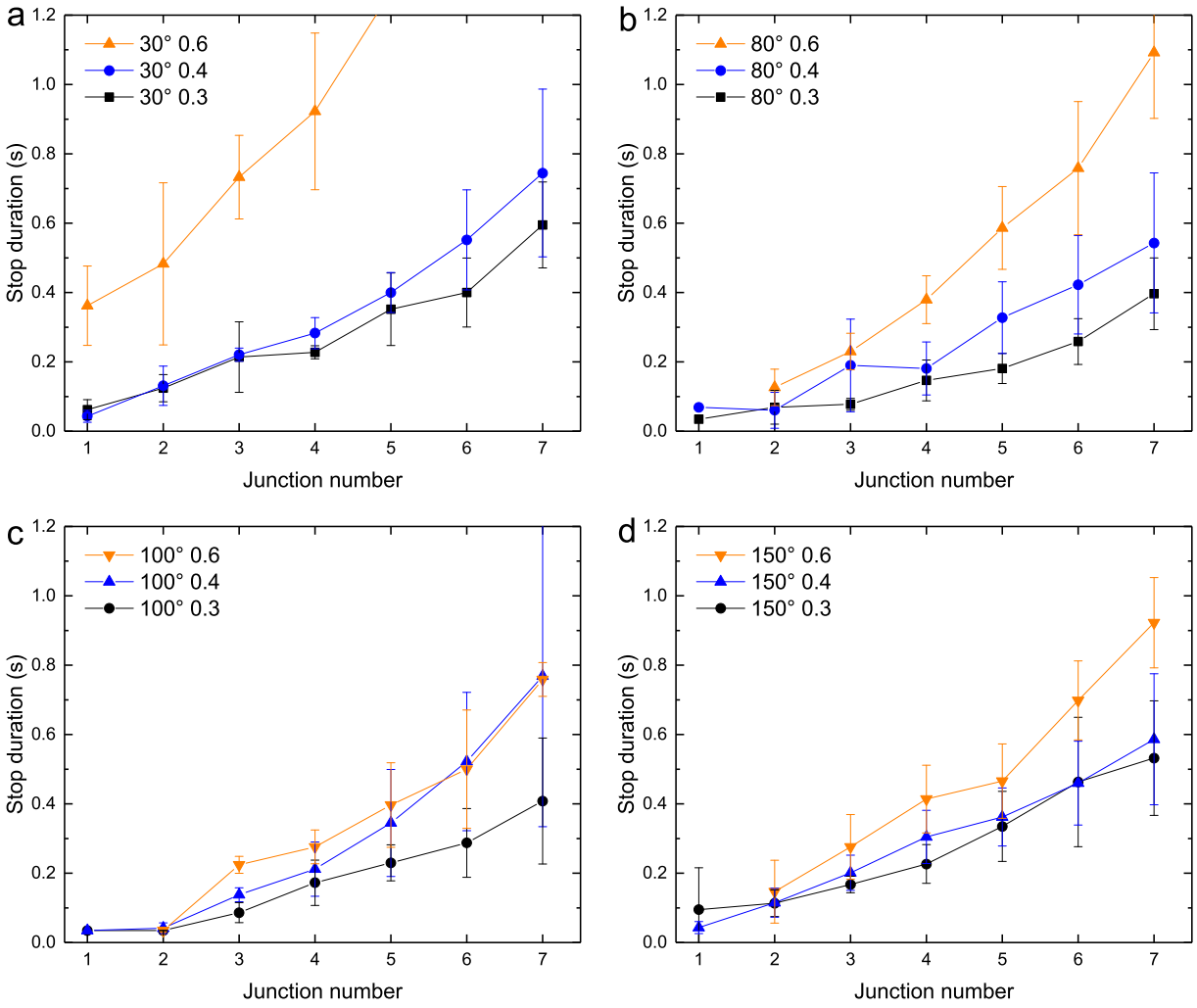

Fig. 8. Stopping duration of the liquid in a main channel having branches 0.3, 0.4, and 0.6 mm wide and angles of (a) 30°, (b) 80°, (c) 100°, and (d) 150°.

stopping time. Apart from side channels having a width of 0.6 mm, the dynamics of the main channel with side channels 0.4 and 0.3 mm wide with tilting angles of 30°, 80°, 100°, and 150° were analysed. Specifically, we studied whether the stopping duration was influenced by the angles and widths of the branches. In Fig. 8, the stopping duration at each junction is plotted for the angles indicated in the figure. As in Fig. 5, the mean stopping duration increased with the junction number, which happened regardless of the side-channel width and angle.

As anticipated, the widest side channels of 0.6 mm resulted in the longest stopping times and the smallest side channels, 0.3 mm, caused the shortest stops in the experiments, irrespective of the tilting angle. Fig. 7 shows that the liquid stopped for a considerable time right at the edge of the junction before it started filling the side channels. The higher capillary pressure in smaller channels means that the liquid can enter the side channels faster than it does in wider side channels, causing decreased stopping times. Transferring our results to a porous system suggests that the liquid enters smaller channels before bigger ones are filled, taking a preferred pathway.

In our investigations, it was not clear whether the liquid stopped until the whole side channel was completely filled or whether it had already resumed flowing before that; various experiments revealed slightly divergent behaviour, which would be a matter for further studies.

Again, very low angles had high stopping times. Among the tested angles, 30° with a side channel width of 0.6 mm was associated with considerably greater stopping durations than were all other tested angles (30°, 80°, 100°, and 150°) and channel widths (0.3, 0.4, and 0.6 mm). It can be concluded that the liquid is influenced the most if the side channel has a low tilting angle; above a certain critical angle, the width of the side channel plays a bigger role.

4. Conclusions

This study systematically investigated how a wetting liquid moves in a soft porous system and we hypothesize that the capillary flow speed can be tailored in a model system of microchannels by the angle, size and position of attached side channels. Previous studies concerned capillary flow in hard materials such as glass or silicon wafers [9,11,12] even though it is known that the behaviour is different on soft substrates [26–28]. A 2D structure was designed using a quick, simple, and cost-effective method that involves the CAD design and 3D printing of a mould, and the casting/curing of gel in the mould. The gel that was finally peeled off the mould contained defined μ-channels. The method presented is flexible in terms of both geometric variation and choice of material in comparison to other commonly used methods which are more costly and time consuming [9,11,12,14].

Similar to the results of [14] the liquid in the main channel displayed a stick–slip motion in that it became pinned and depinned at junctions with a side channel on one or both sides of the main channel. Furthermore, the stopping time increased with low tilting angles and large side-channel widths, which gives rise to that smaller pores are filled first in a porous system. Longer stopping times were measured towards the end of the capillary, proportional to the decreased flow speed in the main channel. Because of the discontinuous movement, inertia is hypothesised to play a large role in the branched-channel systems studied here and might also explain why no permanent pinning was observed in contrast to [14], where the structures had smaller dimensions. This paper confirms the existence of preferred pathways taken by imbibing liquids and illustrates how to control the flow by manipulating the geometric design. The findings presented can further have impact on paper-based medical devices by adjusting the speed of test liquid by the geometrical paper structure of the device and so improving the specificity and sensitivity. The present results are also expected to be applicable to foams, as well as lab-on-a-chip diagnostics using gels. Furthermore, the testing set-up is relevant to biological contexts.

A future study should investigate for instance how and if the stopping time is related to the length, volume or amount of side channels. Another interesting aspect to study is the impact of inertia in various sizes while having the same geometry.

Acknowledgements

The financial support from the VINN Excellence Center, SuMo BIOMATERIALS, is acknowledged as is the financial contribution from VINNMER for AS.

References

[1] X. Li, D.R. Ballerini, W. Shen, A perspective on paper-based microfluidics: current status and future trends, Biomicrofluidics 6 (1) (2012) 011301.
[2] Y. Nonomura, Y. Morita, T. Hikima, E. Seino, S. Chida, H. Mayama, Spreading behavior of water droplets on fractal agar gel surfaces, Langmuir 26 (20) (2010) 16150–16154.
[3] J. Hu, S. Wang, L. Wang, F. Li, B. Pingguan-Murphy, T.J. Lu, F. Xu, Advances in paper-based point-of-care diagnostics, Biosensors Bioelectron. 54 (2014) 585–597.
[4] L.R. Fisher, P.D. Lark, An experimental study of the washburn equation for liquid flow in very fine capillaries, J. Colloid Interface Sci. 69 (3) (1979) 486–492.
[5] R. Lucas, Ueber das Zeitgesetz des kapillaren Aufstiegs von Flüssigkeiten, Kolloid-Zeitschrift 23 (1) (1918) 15–22.
[6] E.W. Washburn, The dynamics of capillary flow, Phys. Rev. 17(3) (1921) 273–283.
[7] A.B.D. Cassie, S. Baxter, Wettability of porous surfaces, Transa. Faraday Soc. 40 (1944) 0546–0550.
[8] R.N. Wenzel, Resistance of solid surfaces to wetting by water, Ind. Eng. Chem. 28 (8) (1936) 988–994.
[9] R.R. Rye, F.G. Yost, J.A. Mann, Wetting kinetics in surface capillary grooves, Langmuir 12 (20) (1996) 4625–4627.
[10] L.A. Romero, F.G. Yost, Flow in an open channel capillary, J. Fluid Mech. 322 (1996) 109–129.
[11] D. Yang, M. Krasowska, C. Priest, M.N. Popescu, J. Ralston, Dynamics of capillary-driven flow in open microchannels, J. Phys. Chem. C 115 (38) (2011) 18761–18769.
[12] Y. Chen, L.S. Melvin, S. Rodriguez, D. Bell, M.M. Weislogel, Capillary driven flow in micro scale surface structures, Microelectr. Eng. 86 (4–6) (2009) 1317–1320.
[13] M.L. Blow, H. Kusumaatmaja, J.M. Yeomans, Imbibition through an array of triangular posts, J. Phys: Condens. Matter 21 (46) (2009) 464125.
[14] J. Feng, J.P. Rothstein, One-way wicking in open micro-channels controlled by channel topography, J. Colloid Interface Sci. 404 (2013) 169–178.
[15] C.J. Ridgway, P.A.C. Gane, J. Schoelkopf, Effect of capillary element aspect ratio on the dynamic imbibition within porous networks, J. Colloid Interface Sci. 252 (2) (2002) 373–382.
[16] J. Schoelkopf, P.A.C. Gane, C.J. Ridgway, Observed non-linearity of Darcy-permeability in compacted fine pigment structures, Colloids Surfaces A: Physicochem. Eng. Asp. 236 (1) (2004) 111–120.
[17] J. Schoelkopf, P.A.C. Gane, C.J. Ridgway, G.P. Matthews, Practical observation of deviation from Lucas-Washburn scaling in porous media, Colloids Surfaces A: Physicochem. Eng. Asp. 206 (1) (2002) 445–454.
[18] J. Bico, D. Quéré, Precursors of impregnation, EPL (Europhysics Letters) 61 (3) (2003) 348.
[19] H. Aslannejad, S.M. Hassanizadeh, Study of hydraulic properties of uncoated paper: image analysis and pore-scale modeling, Transp. Porous Media 120 (1) (2017) 67–81.
[20] J. Schoelkopf, C.J. Ridgway, P.A.C. Gane, G.P. Matthews, D.C. Spielmann, Measurement and network modeling of liquid permeation into compacted mineral blocks, J. Colloid Interface Sci. 227 (1) (2000) 119–131.
[21] C.K. Camplisson, K.M. Schilling, W.L. Pedrotti, H.A. Stone, A.W. Martinez, Two-ply channels for faster wicking in paper-based microfluidic devices, Lab A Chip 15 (23) (2015) 4461–4466.
[22] P.A.C.G. Joachim Schoelkopf, Cathy J. Ridgway, A.G. Omya, Oftringen, Switzerland, G. Peter Matthews, Influence of inertia on liquid absorption into paper coating structures, Nordic Pulp & Paper Res. J. 15 (2000) 422–430.
[23] W.B. Haines, Studies in the physical properties of soils: IV. A further contribution to the theory of capillary phenomena in soil, J. Agri. Sci. 17 (1927) 264–290.
[24] A.K. Yetisen, M.S. Akram, C.R. Lowe, Paper-based microfluidic point-of-care diagnostic devices, Lab A Chip 13 (12) (2013) 2210–2251.

[25] D. Kaneko, H. Furukawa, Y. Tanaka, Y. Osada, J.P. Gong, Flower petal-like pattern on soft hydrogels during vodka spreading, in: Z.D. Hórvölgyi, É. Kiss (Eds.), Colloids for Nano- and Biotechnology, Springer, Berlin Heidelberg, Berlin, Heidelberg, 2008, pp. 225–230.
[26] M.E.R. Shanahan, A. Carré, Viscoelastic dissipation in wetting and adhesion phenomena, Langmuir 11 (1995) 1396–1402.
[27] S.J. Park, B.M. Weon, J.S. Lee, J. Lee, J. Kim, J.H. Je, Visualization of Asymmetric Wetting Ridges on Soft Solids with X-ray Microscopy, 5 (2014) 4369.
[28] L. Chen, E. Bonaccurso, T. Gambaryan-Roisman, V. Starov, N. Koursari, Y. Zhao, Static and dynamic wetting of soft substrates, Curr. Opinion Colloid & Interface Sci. 36 (2018) 46–57.
[29] J. Andersson, A. Strom, T. Geback, A. Larsson, Dynamics of capillary transport in semi-solid channels, Soft Matter 13 (14) (2017) 2562–2570.
[30] X. Zhang, L. Li, C. Luo, Gel integration for microfluidic applications, Lab a Chip 16 (10) (2016) 1757–1776.
[31] B.J. Taylor, A. Howell, K.A. Martin, D.P. Manage, W. Gordy, S.D. Campbell, S. Lam, A. Jin, S.D. Polley, R.A. Samuel, A. Atrazhev, A.J. Stickel, J. Birungi, A.K. Mbonye, L.M. Pilarski, J.P. Acker, S.K. Yanow, A lab-on-chip for malaria diagnosis and surveillance, Malaria J. 13 (1) (2014) 179.
[32] J.E. Silva, R. Geryak, D.A. Loney, P.A. Kottke, R.R. Naik, V.V. Tsukruk, A.G. Fedorov, Stick-slip water penetration into capillaries coated with swelling hydrogel, Soft Matter 11 (29) (2015) 5933–5939.
[33] E. Hermansson, E. Schuster, L. Lindgren, A. Altskär, A. Ström, Impact of solvent quality on the network strength and structure of alginate gels, Carbohyd. Polym. 144 (2016) 289–296.
[34] E. Schuster, J. Eckardt, A.-M. Hermansson, A. Larsson, N. Loren, A. Altskar, A. Strom, Microstructural, mechanical and mass transport properties of isotropic and capillary alginate gels, Soft Matter 10 (2) (2014) 357–366.
[35] M. Davidovich-Pinhas, H. Bianco-Peled, A quantitative analysis of alginate swelling, Carbohyd. Polym. 79 (4) (2010) 1020–1027.
[36] H. Kusumaatmaja, C.M. Pooley, S. Girardo, D. Pisignano, J.M. Yeomans, Capillary filling in patterned channels, Phys. Rev. E 77 (6) (2008) 067301.
[37] S. Girardo, S. Palpacelli, A. De Maio, R. Cingolani, S. Succi, D. Pisignano, Interplay between shape and roughness in early-stage microcapillary imbibition, Langmuir 28 (5) (2012) 2596–2603.
[38] W. Liu, Y. Li, Y. Cai, D.P. Sekulic, Capillary rise of liquids over a microstructured solid surface, Langmuir 27 (23) (2011) 14260–14266.
[39] R.R. Rye, F.G. Yost, E.J. O'Toole, Capillary flow in irregular surface grooves, Langmuir 14 (14) (1998) 3937–3943.
[40] N.R. Tas, J. Haneveld, H.V. Jansen, M. Elwenspoek, A.V.D. Berg, Capillary filling speed of water in nanochannels, Appl. Phys. Lett. 85 (15) (2004) 3274–3276.
[41] C.H. Bosanquet, LV.On The Flow of Liquids into Capillary Tubes, Philosophical Magazine Series 6 45(267) (1923) pp. 525–531.